

NANO-FLUID EFFECTS ON TOTAL ENTROPY GENERATION THROUGH PLATE HEAT EXCHANGERS

M. Samy Hefny, A. Taher Hussein, A. Mostafa Hamed, N. A. Mahmoud

Department of Mechanical power Engineering, Ain Shams University, Faculty of Engineering, Cairo, Egypt.

Nomenclature

A	Total surface area (m ²)	\dot{m}	Mass flow rate (Kg/sec)
c_p	Specific heat capacity (J/kg K)	N_c	Number of channels for cold or hot streams
D_p	Port diameter (mm)	S	Entropy (W/K)
H	Depth of corrugation (mm)	t	Plate thickness (mm)
k_w	Thermal conductivity of plate material (W/m K)	T	Temperature (°C)
L_h	Horizontal distance between center of ports (mm)	W	Plate width inside gasket (mm)
L_v	Vertical distance between center of ports (mm)	\dot{V}	Volume flow rate (LPM)

Greek Letters

β	Chevron angle (°)	Δ	Change
ρ	Density (kg/m ³)		

Subscript

c	cold	i	inlet
gen	generation	nf	Nano-fluid
h	hot	o	outlet

Abbreviations

CSP	Concentrated Solar Power
HTC	Heat Transfer Coefficient
HTF	Heat Transfer Fluid
MWCNT	Multi-Walled Carbon Nano-Tubes
DI	De-Ionized
LPM	Liter Per Minute

ABSTRACT

A comparative study and results analysis performed for evaluating the entropy generation through corrugated plate heat exchanger by using Nano particles of MWCNT dispersed in DI water, using three different concentrations of MWCNT of 0.25 g/liter, 0.5 g/liter and 1 g/liter. Besides, the variation of the hot Nano-DI water inlet temperature at $T_{h,i} = 50^\circ\text{C}$, 60°C , 70°C and 80°C ; by varying the volume flow rate of the hot Nano-DI water side at $\dot{V}_h = 1$ LPM, 2 LPM, 3 LPM, 4LPM and 5 LPM, and varying volume flow rate of the cold water side at $\dot{V}_c = 1$ LPM, 2 LPM, 3 LPM, 4LPM and 5 LPM. The total entropy generation " S_{gen} " increases with the increase of the volume flow rate of the hot fluid side. Moreover, the total entropy generation increases by increasing the inlet temperature of the hot fluid side. Moreover, the total entropy generation decreases with decreasing the volume flow rates of the cold fluid side. Also, the total entropy generation increases by increasing the Nano particles concentration in the DI water, except for the 0.5 g/liter, it shows lower values for the total

entropy generation. However, the 1 g/liter Nano-DI water reaches 155% increase over the DI water, at 80°C.

INTRODUCTION:

A lot of applications involve continuous processes of heating and cooling, such as: power generation, refrigeration and air conditioning, microelectronics, heat pipes, etc. Considering the rapid increase in energy demand, decreasing energy loss due to ineffective use, has become an important task in present time. Moreover, a reduction in energy consumption is possible by enhancing the performance of such systems that involve heat which has major effect on carbon footprints as well. There is a real desire to enhance the efficiency of heat transfer through the heat exchangers, which will lead to reduction of the sizes of such equipment and accordingly, the associated costs of production, operation and power consumption. This can be achieved in many ways, such as: modifying fluid properties, surface shape, roughness, attaching objects to increase surface area and turbulences (Wen et al., 2009). The most frequently used working fluids or coolants through the heat exchangers are: water, ethylene glycol, engine oil, refrigerants. However, the heat transfer ability is limited by the working fluid transport properties. One of the methods for heat transfer enhancement is the application of additives to the working fluids to change the fluid transport properties and flow features. One of the most important parameters in the heat transfer process, to achieve energy efficient heat exchanger, is the thermal conductivity "k" of the working fluid, which is relatively low when compared to the thermal conductivity of solids, in general, which have much higher thermal conductivities than fluids. Due to the giant improvements in Nanotechnology, it becomes possible to produce solid particles within the nanometer sizes (<100 nm). Hence, an innovative idea of dispersing Nano particles into base fluids was proposed, to produce liquid suspensions, which are called "**Nanofluids**", to use them in heat transfer enhancement of working fluids, as they can improve the effective thermal conductivity of working fluids, which was proposed first by Masuda et al. 1993 and Choi et al. 1995. Therefore, the potential benefits of Nano fluids could provide intensive performance, size/weight, and cost advantages. From here came the idea to disperse nanoparticles into DI water to enhance its thermal conductivity behavior to improve the convective heat transfer through heat exchangers. The type of base fluid used in this research is "**De-Ionized Water**", as it is used in capturing solar energy in solar collectors' applications. So, the main objective of the current study is, to show the effect of nanofluids on entropy generation, experimentally in heat exchangers, causing the reduction in area of heat transfer needed and pumping power. (Huang et al, 2016) studied the effect of using hybrid nanofluid mixture, as a hot fluid, of 1.89% volume fraction of Al₂O₃/water and 0.0111% volume fraction of MWCNT/water, mixed at volume ratio of 2.5:1, experimentally on pressure drop and heat transfer properties in a plate heat exchanger with chevron corrugations. The hybrid nanofluid had slightly higher heat transfer coefficient than that of Al₂O₃/water nanofluid and water, at the same flow velocity, due to the small added amount of MWCNT, and the pressure drop of hybrid nanofluid was smaller than that of Al₂O₃/water nanofluid, and slightly higher than that of water. (Safi et al, 2014) examined experimentally the convective heat transfer properties of MWCNT-TiO₂/water hybrid nanofluid, as hot stream, flowed through plate heat exchanger at various concentrations (from 0.02 to 0.08 wt. %) and temperatures (from 36 to 60 °C) and volume flow rates of hot fluid from (2 to 3.5 LPM). Results showed that the heat transfer coefficient increased with increasing the mass fraction and volume flow rate of nanofluid, and with decreasing the inlet temperature of hot nanofluid. (Kabeel et al, 2013) examined experimentally the laminar convective heat transfer coefficient, heat transfer rate, pressure drop and effectiveness of Al₂O₃/water nanofluid, as hot stream, flowed through corrugated plate heat exchanger at various volume concentrations (from 1 to 4%). Results showed that effectiveness decreased. The heat transfer coefficient increased with increasing nanoparticles volume fraction and Reynolds number of nanofluid, and reached 13% enhancement, at 4% volume fraction, at constant Reynolds number, with 9.8% uncertainty. Moreover, pressure drop increased by 45%, and pumping power rose by 95% over the base fluid, at 4% volume fraction. They were doubt about results of nanofluids in their research and concluded that 2% volume fraction would be optimum considering heat transfer enhancement with respect to pumping power rise.

• **Methodology:**

In the present research, it is targeted to investigate experimentally the entropy generation of hot stream of MWCNT / DI water, at mass concentrations of 0.25 g/liter, 0.5 g/liter and 1 g/liter, and at various inlet temperatures of 50 °C, 60 °C, 70 °C and 80 °C, through counter flow arrangement in corrugated plate heat exchanger, for evaluating the performance of using Nano particles of MWCNT dispersed in DI water, by varying the volume flow rate of the hot Nano-DI water side at $\dot{V}_h = 1 \text{ LPM}, 2 \text{ LPM}, 3 \text{ LPM}, 4 \text{ LPM}$ and 5 LPM , and varying volume flow rate of the cold water side at $\dot{V}_c = 1 \text{ LPM}, 2 \text{ LPM}, 3 \text{ LPM}, 4 \text{ LPM}$ and 5 LPM .

• **Nano-DI water preparation:**

In the current research, DI water is used as the base fluid, in which nanoparticles are dispersed. Moreover, MWCNTs purchased from (Nanotech Egypt Inc., Egypt) with 10 nm diameter and 100 nm length, are used as the nanoparticles.

MWCNT/ DI water is prepared using Ultrasonicator, (Hielscher, Ultrasound technology Inc., Germany) existed in (Excellence Center of Science & Technology, Egypt), to prepare mass concentrations of 0.25 g/liter, 0.5 g/liter and 1 g/liter by dispersing the required mass of MWCNT, into the available mass of DI water. Figures (1, a and b) show preparation of MWCNT/ DI water using Ultrasonicator and the TEM photo of MWCNT/ DI water, prepared Nano-fluid.

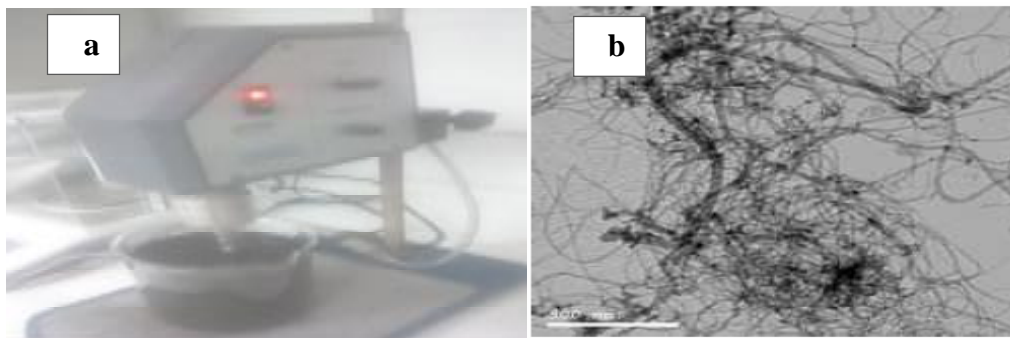


Figure (1, a and b): preparation of MWCNT/ DI water using Ultrasonicator and the TEM photo of MWCNT/ DI water.

• **Nano-DI water thermo-physical properties:**

The specific heat capacity " $c_{p,nf}$ " is measured by differential scanning calorimetry technique (DSC Q2000, TA instruments Inc., England). Moreover, the density " ρ_{nf} " is measured by weighing the mass of known volume of the prepared Nano-DI water. Table (1) shows the measured thermo-physical properties of MWCNT/ DI water at various mass concentrations and temperatures.

Table (1): Thermo-physical properties for MWCNT/ DI water.

Nano-DI water	Mass concentration (g/liter)	T (°C)	ρ_{nf} (kg/m ³)	$c_{p,nf}$ (J/kg K)
MWCNT / DI water	1	50	1049.976	6439.5
		60	1047.091	7295.38
		70	1045.168	8346.53
		80	1042.283	10027.5
	0.5	50	1018.994	5815.09
		60	1016.051	6654.3
		70	1014.090	7644.48
		80	1011.147	8649.7
	0.25	50	1003.498	5502.89
		60	1000.527	6333.76
		70	998.546	7293.45

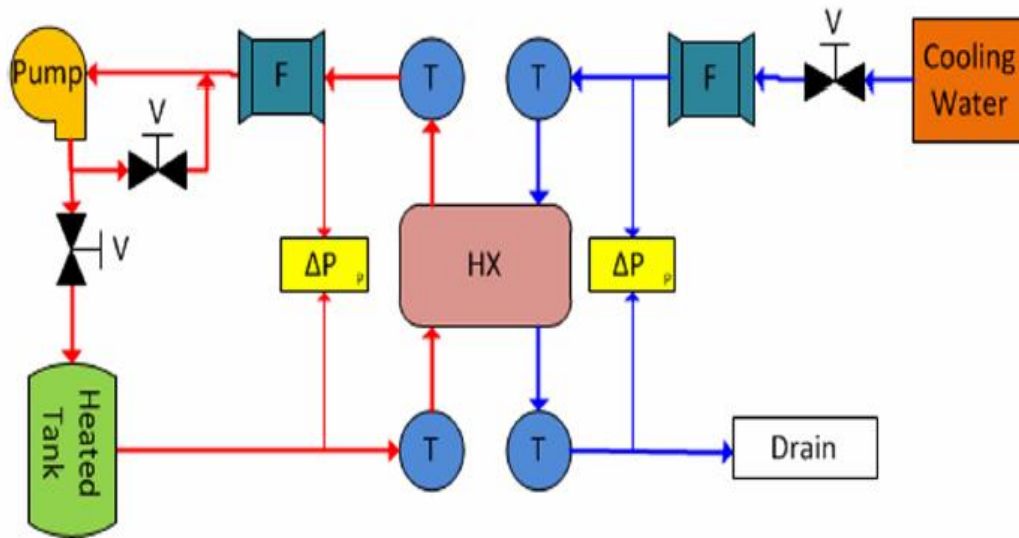


Figure (3): Line diagram for the experimental test setup

The hot fluid stream is the Nano-DI water loop and the cold fluid stream is the tap water loop. The Nano-DI water is stored in 5 liters stainless steel tank, with four, 2.5 KW each, immersed electric heaters, to heat the Nano-DI water. The desired inlet temperature of the hot Nano-DI water to the heat exchanger is controlled by a digital thermostat and by using Variac of 2.5 kw. The Nano-DI water is drawn by a gear pump and pumped through the plate heat exchanger, on the hot stream side of it, and then, back to the tank. The volume flow rate of the hot Nano-DI water is measured at the hot stream outlet port of the heat exchanger, using visual indication rotameter.

The cold water is stored in 10 liters plastic tank. . The inlet temperature of the cold water to the heat exchanger varies between 25 °C and 30 °C, as it comes from the main grid. The cold water is drawn by a centrifugal pump and pumped through the plate heat exchanger on the cold stream side of it, and then, back to the drain. The volume flow rate of the cold water is measured at the cold stream inlet port of the heat exchanger, using visual indication rotameter. The inlet and outlet temperatures from the heat exchanger for the hot and cold streams are measured immediately at the entrance and exit ports of the heat exchanger, using four water-proof temperature sensors.

• **Test procedure:**

For the selected mass concentration of the Nano-DI water sample either to be 0.25 g/liter, 0.5 g/liter or 1 g/liter. The desired inlet temperature of the hot Nano-DI water to the heat exchanger inlet port S1 is preset, using the digital thermostat and Variac, at 50 °C, 60 °C, 70 °C and 80 °C, for each separate test run. While the inlet temperature of the cold water to the inlet port S3, comes from city water, changes between 25 °C and 30 °C during all test runs. Then the volume flow rate of the hot Nano-DI water stream is varied, using Inverter, at 1, 2, 3, 4 and 5 LPM, for each separate test run. While varying the volume flow rate of the cold water stream, using valve, at 1, 2, 3, 4 and 5 LPM, for the selected volume flow rate of the hot stream. Upon reaching steady state equilibrium conditions, the outlet temperatures, of the hot Nano-DI water are measured using the water-proof temperature sensors.

• **Thermodynamics and heat transfer analysis:**

The mass flow rates of the Nano-DI water and the cold water through heat exchanger can be calculated from Eq.(1) and Eq.(2), respectively.

$$\dot{m}_{nf} = \rho_{nf} \cdot \dot{V}_{nf} \tag{Eq.(1)}$$

$$\dot{m}_c = \rho_c \cdot \dot{V}_c \tag{Eq.(2)}$$

The entropy change for the hot stream of Nano-DI water and the cold water through heat exchanger paths can be obtained from Eq.(3) and Eq.(4), respectively.

$$\Delta S_{nf} = \dot{m}_{nf} \cdot (s_{nf,o} - s_{nf,i}) = \dot{m}_{nf} \cdot c_{p,nf} \cdot \ln \left(\frac{T_{nf,o}}{T_{nf,i}} \right) \quad \text{Eq.(3)}$$

$$\Delta S_c = \dot{m}_c \cdot (s_{c,o} - s_{c,i}) = \dot{m}_c \cdot c_{p,c} \cdot \ln \left(\frac{T_{c,o}}{T_{c,i}} \right) \quad \text{Eq.(4)}$$

Hence, the total entropy generation for the heat exchanger can be calculated from Eq.(5).

$$\dot{S}_{gen} = \Delta S_{nf} + \Delta S_c \quad \text{Eq.(5)}$$

Figure (4) shows the thermal entropy profile for the hot and cold streams in a counter flow corrugated plate heat exchanger.

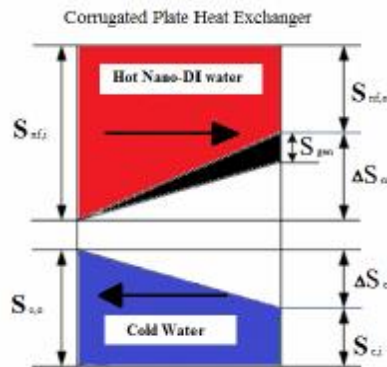


Figure (4): Entropy thermal profile for counter flow plate heat exchanger.

Total entropy generation "S_{gen}" results and analysis:

Figure (5) shows the variation of the total entropy generation through the heat exchanger for the DI water at a) $\dot{V}_c = 5$ LPM, b) $\dot{V}_c = 4$ LPM, c) $\dot{V}_c = 3$ LPM, d) $\dot{V}_c = 2$ LPM and e) $\dot{V}_c = 1$ LPM, it is noticed that the total entropy generation increases, with the increase of the volume flow rate of the hot fluid side. Moreover, the total entropy generation increases, by increasing the inlet temperature of the hot fluid side. Moreover, the total entropy generation decreases with decreasing the volume flow rates of the cold fluid side. The same behavior was observed for the three different concentrations of 0.25 g/liter, 0.5 g/liter and 1 g/liter of Nano-DI water in Figures (6), (7) and (8) respectively. Moreover, the total entropy generation increases, by increasing the Nano particles concentration in the DI water, except for the 0.5 g/liter, it shows lower values for the total entropy generation. Figures (9), (10), (11) and (12) show the variation of the total entropy generation at constant inlet temperatures of $T_{h,i} = 50^\circ\text{C}$, 60°C , 70°C and 80°C respectively. The 0.25 g/liter sample showed increase in the total entropy generation at 50°C , over the 0.5 g/liter, but lower than the 1 g/liter sample. Moreover, the increase in total entropy generation increases, with increasing temperature of hot Nano-DI water from 60°C to 80°C , reaching 118% increase over the DI water, at 80°C . Moreover, the increase in total entropy generation decreases, by decreasing the volume flow rate of the cold fluid, at the same hot Nano-DI water inlet temperature. The 0.5 g/liter sample showed decrease in the total entropy generation at 50°C , below the DI water, 0.25 g/liter and 1 g/liter samples. Moreover, the total entropy generation decreases, with decreasing flow rate of the cold water side. However, the total entropy generation increases, with increasing temperature of hot Nano-DI water from 60°C to 80°C , reaching 82% increase over the DI water, at 80°C . However, still lower than the 0.25 g/liter and 1 g/liter samples. The 1 g/liter sample showed the highest increase in the total entropy generation at 50°C , over the DI water, 0.25 g/liter and 0.5 g/liter samples. Moreover, the total entropy generation increases, with increasing temperature of hot Nano-DI water from 60°C to 80°C , reaching 155% increase over the DI water, at 80°C . Moreover, the increase in the total entropy generation decreases, by decreasing volume flow rate of the cold fluid, at the same hot Nano-DI water inlet temperature. The increase of the total entropy generation of the heat exchanger with increasing inlet temperature of the hot Nano-DI water, may be due to the increase of the specific heat property of Nano-DI water with increasing temperature, and due to the increase of external source of irreversibility due to the rise in the temperature difference between the hot and cold sides in the heat exchanger.

1) DI water results:

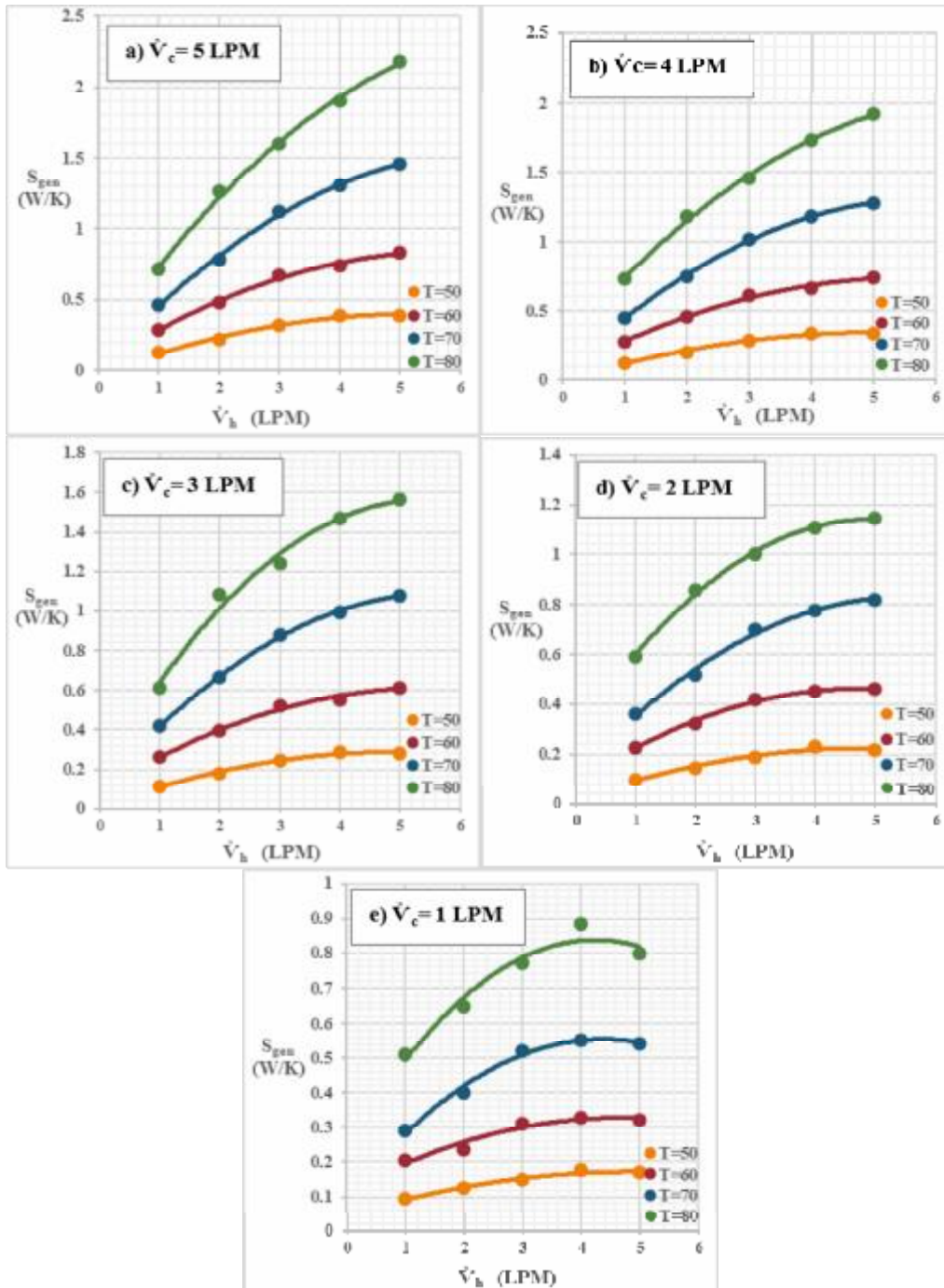


Figure (5): Variation of S_{gen} with volume flow rate of DI water at a) $\dot{V}_c = 5$ LPM, b) $\dot{V}_c = 4$ LPM, c) $\dot{V}_c = 3$ LPM, d) $\dot{V}_c = 2$ LPM and e) $\dot{V}_c = 1$ LPM.

2) Nano-DI water, 0.25 g/liter results:

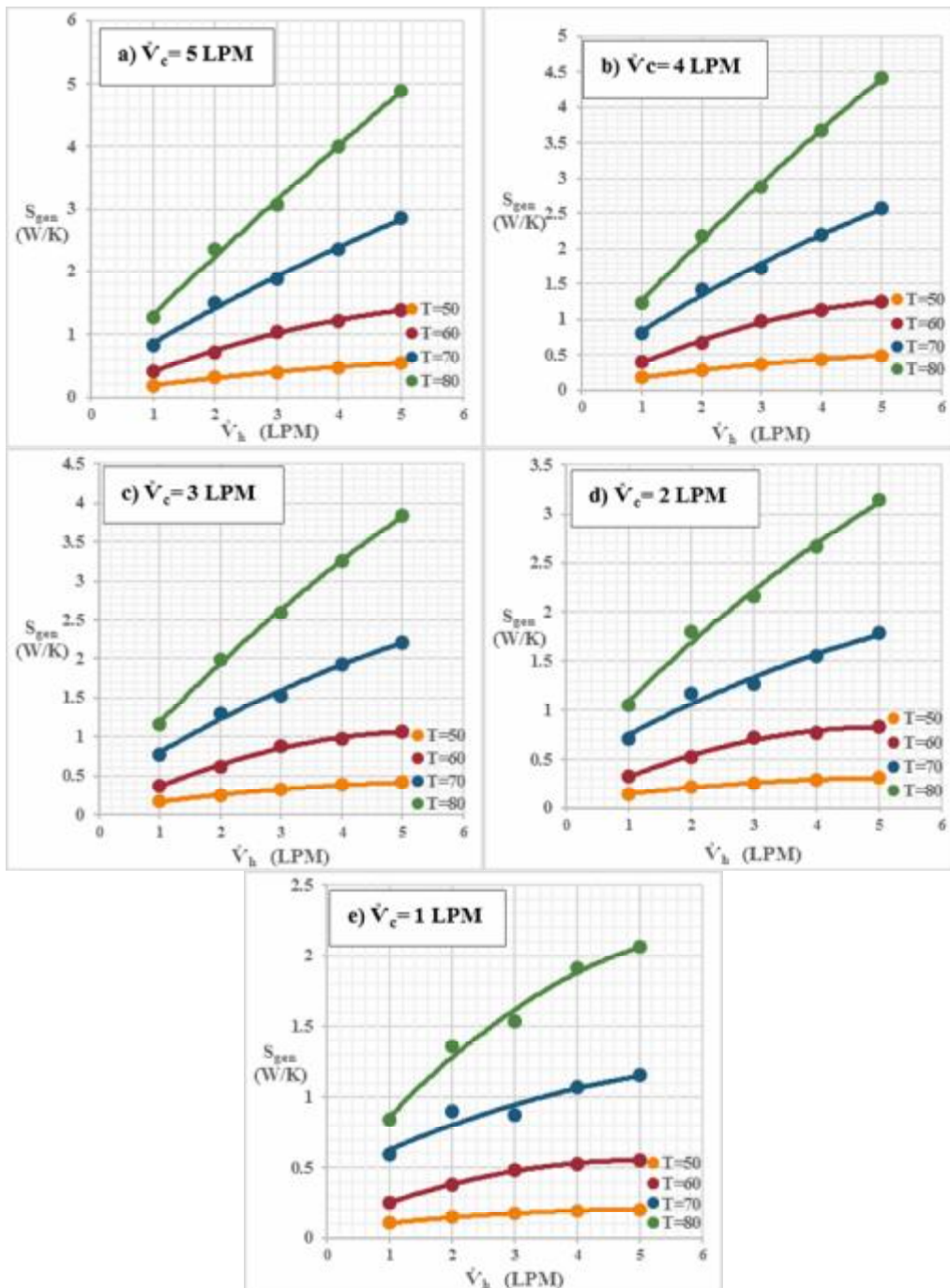


Figure (6): Variation of S_{gen} with volume flow rate of Nano-DI water, 0.25 g/liter, at a) $\dot{V}_c = 5$ LPM, b) $\dot{V}_c = 4$ LPM, c) $\dot{V}_c = 3$ LPM, d) $\dot{V}_c = 2$ LPM and e) $\dot{V}_c = 1$ LPM .

3) Nano-DI water, 0.5 g/liter results:

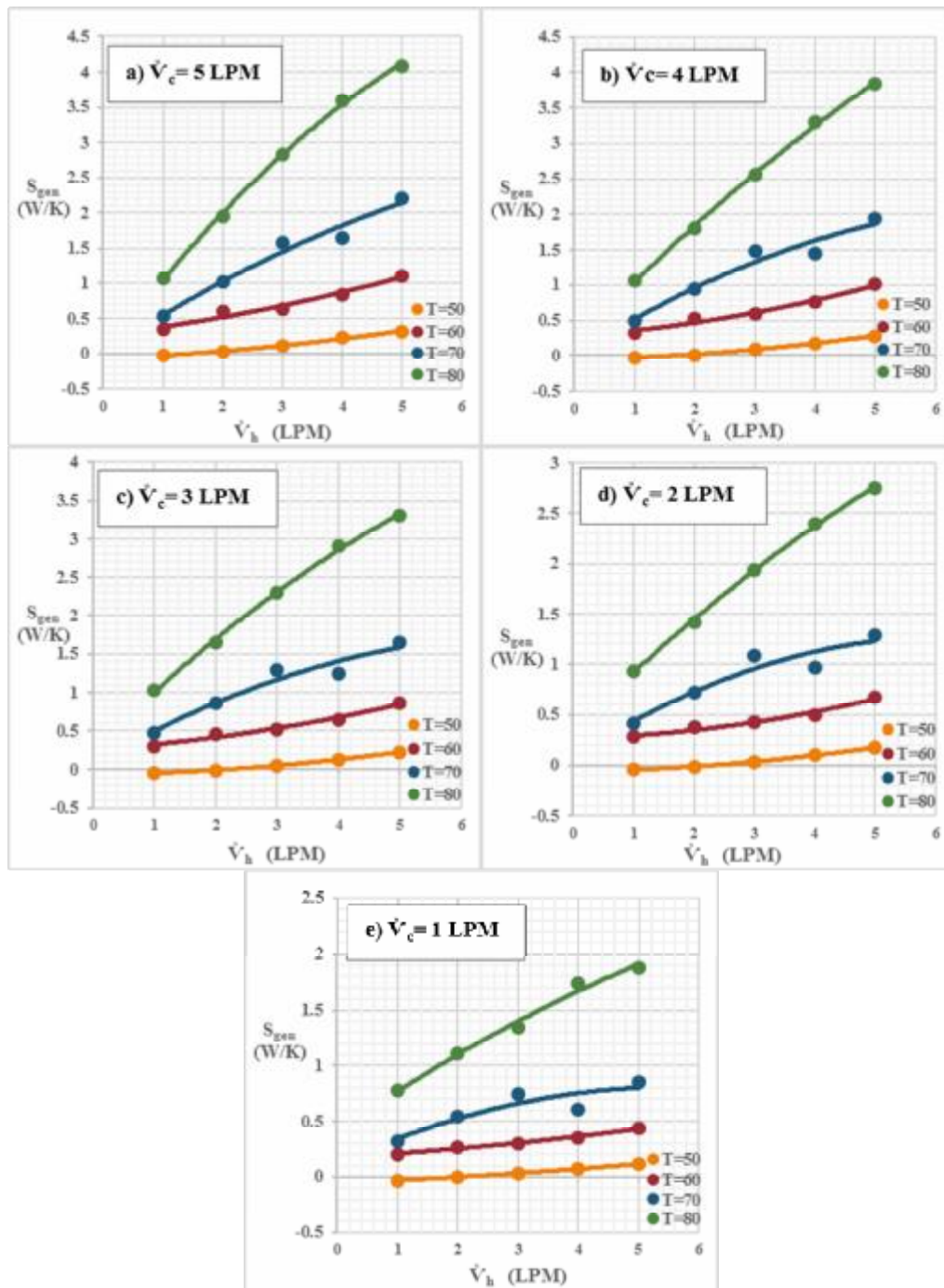


Figure (7): Variation of S_{gen} with volume flow rate of Nano-DI water, 0.5 g/liter, at a) $\dot{V}_c = 5$ LPM, b) $\dot{V}_c = 4$ LPM, c) $\dot{V}_c = 3$ LPM, d) $\dot{V}_c = 2$ LPM and e) $\dot{V}_c = 1$ LPM .

4) Nano-DI water, 1 g/liter results:

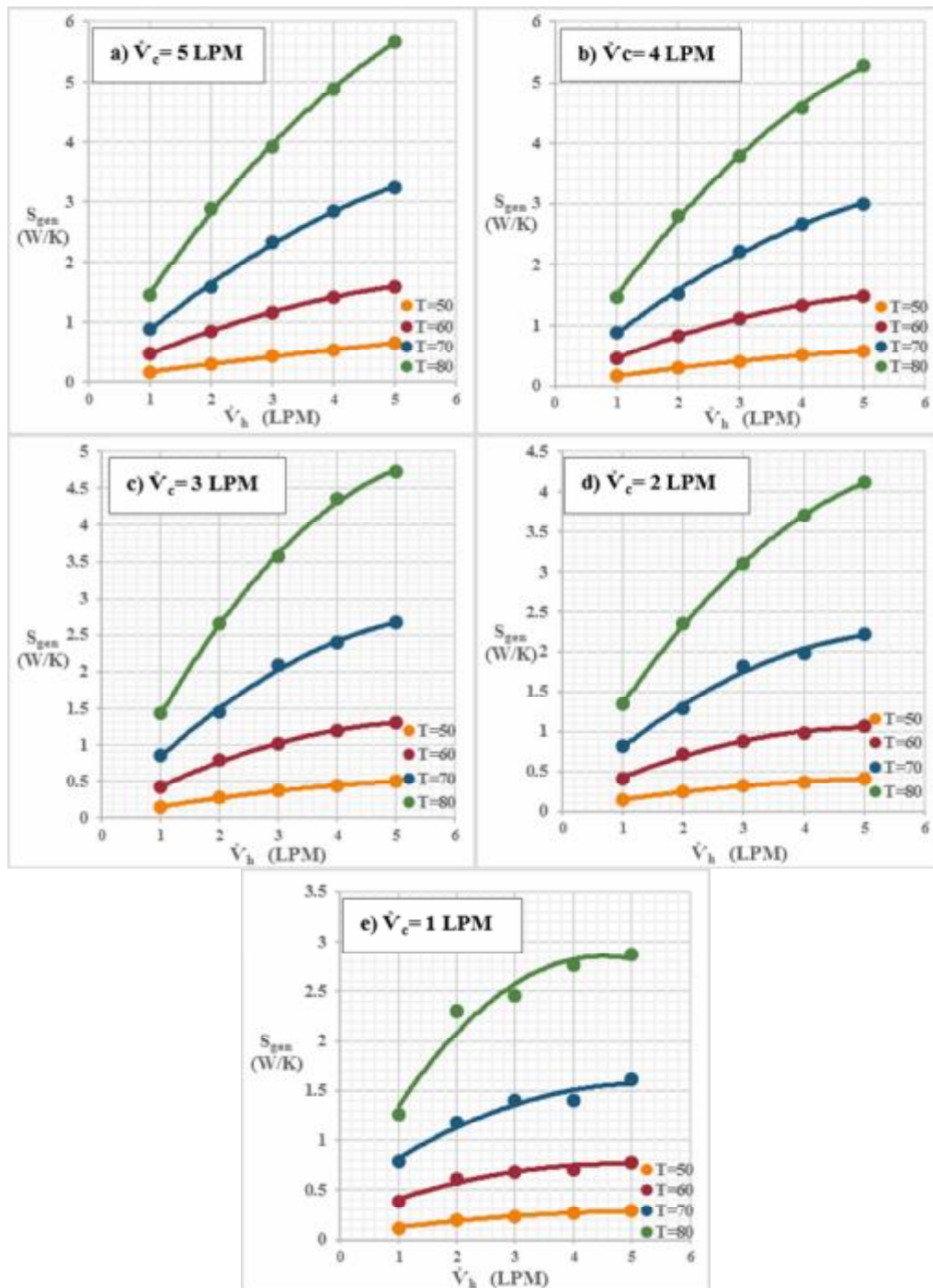


Figure (8): Variation of S_{gen} with volume flow rate of Nano-DI water, 1 g/liter, at a) $\dot{V}_c = 5$ LPM, b) $\dot{V}_c = 4$ LPM, c) $\dot{V}_c = 3$ LPM, d) $\dot{V}_c = 2$ LPM and e) $\dot{V}_c = 1$ LPM .

5) S_{gen} at $T_{h,i}=50\text{ }^{\circ}\text{C}$ results:

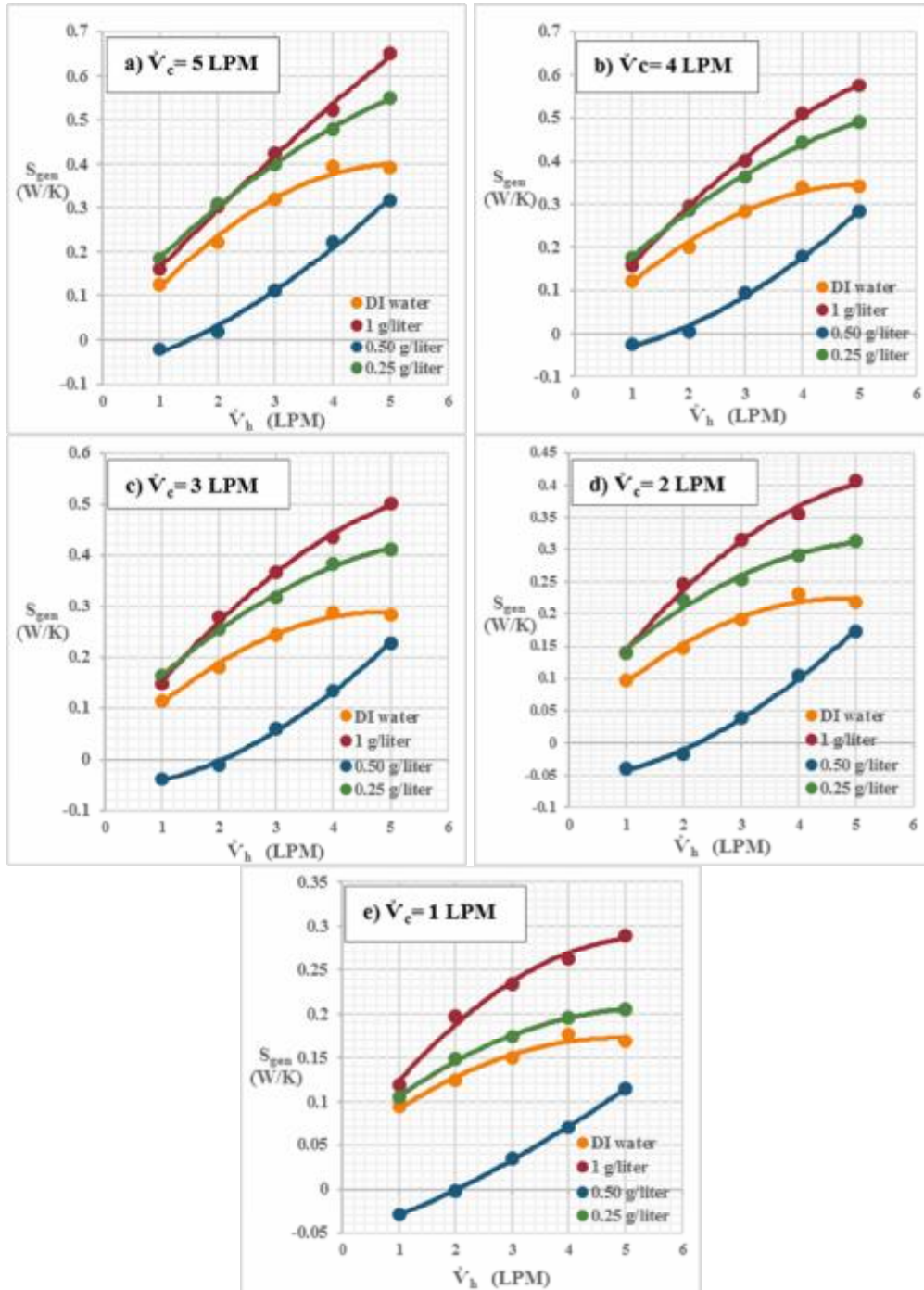


Figure (9): Variation of S_{gen} with volume flow rate of Nano-DI water, at $T_{h,i}=50\text{ }^{\circ}\text{C}$, at a) $\dot{V}_c= 5$ LPM, b) $\dot{V}_c= 4$ LPM, c) $\dot{V}_c= 3$ LPM, d) $\dot{V}_c= 2$ LPM and e) $\dot{V}_c= 1$ LPM.

6) S_{gen} at $T_{h,i}=60\text{ }^{\circ}\text{C}$ results:

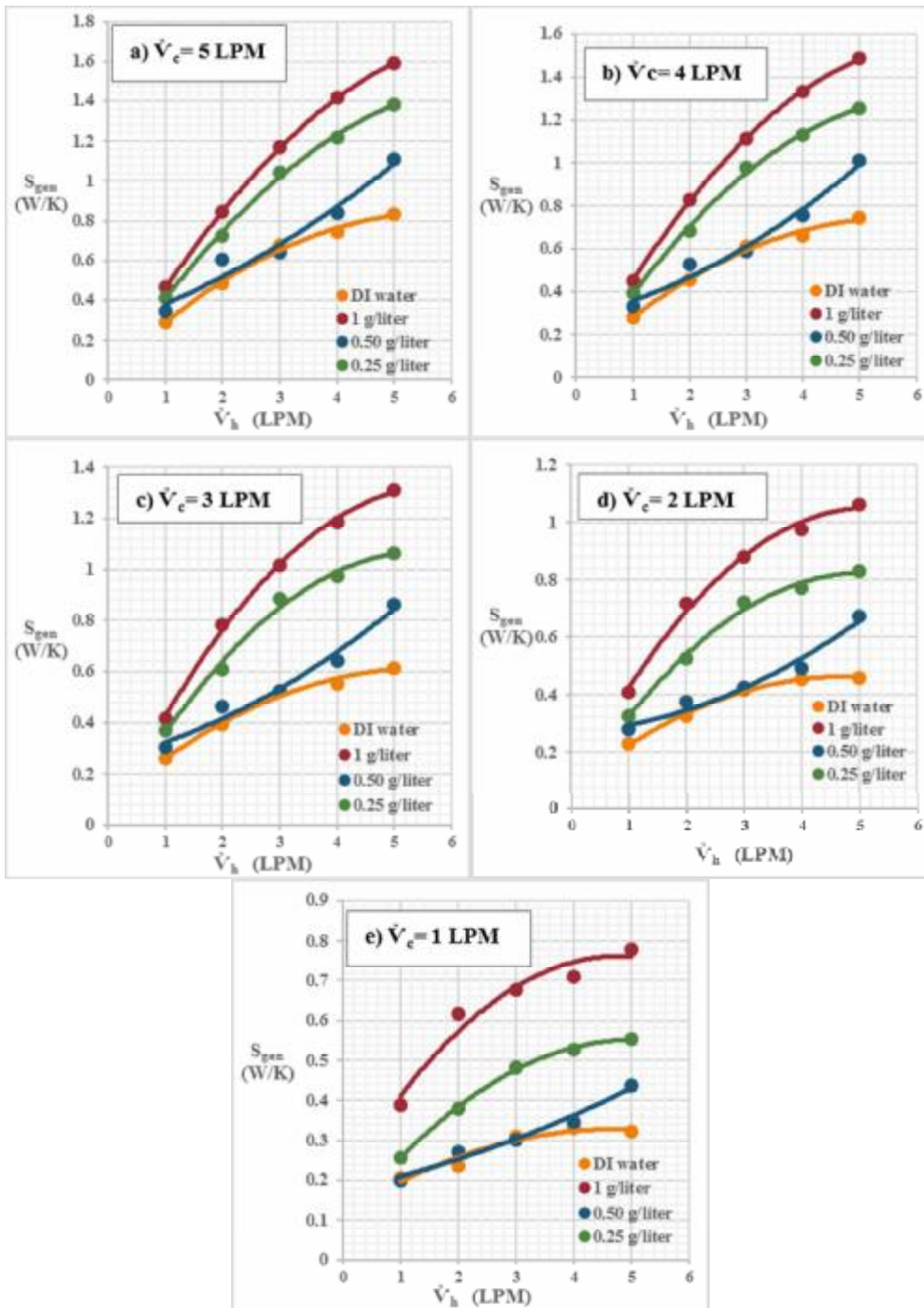


Figure (10): Variation of S_{gen} with volume flow rate of Nano-DI water, at $T_{h,i}=60\text{ }^{\circ}\text{C}$, at a) $\dot{V}_c=5\text{ LPM}$, b) $\dot{V}_c=4\text{ LPM}$, c) $\dot{V}_c=3\text{ LPM}$, d) $\dot{V}_c=2\text{ LPM}$ and e) $\dot{V}_c=1\text{ LPM}$.

7) S_{gen} at $T_{h,i}=70\text{ }^{\circ}\text{C}$ results:

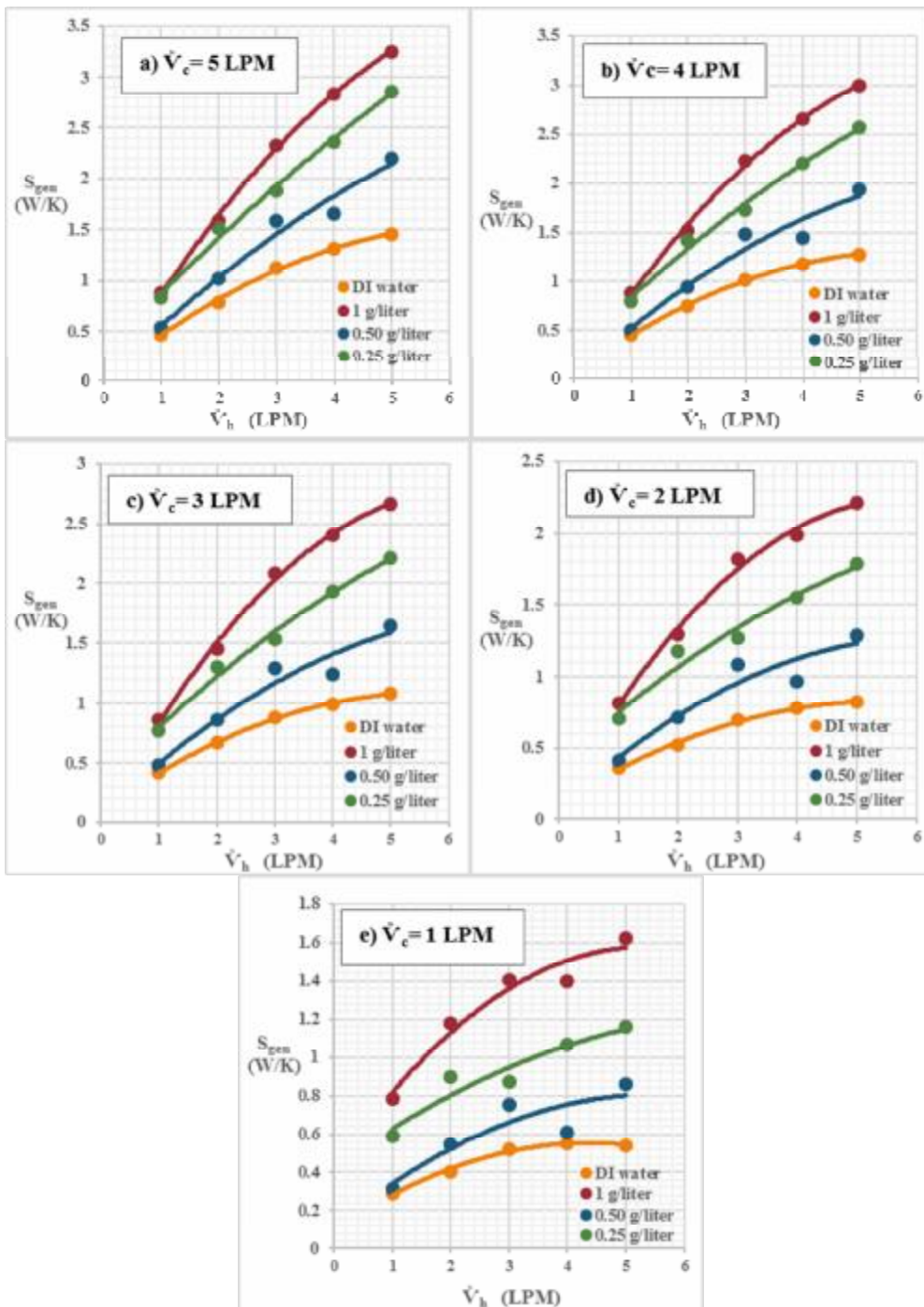


Figure (11): Variation of S_{gen} with volume flow rate of Nano-DI water, at $T_{h,i}=70\text{ }^{\circ}\text{C}$, at a) $\dot{V}_c=5\text{ LPM}$, b) $\dot{V}_c=4\text{ LPM}$, c) $\dot{V}_c=3\text{ LPM}$, d) $\dot{V}_c=2\text{ LPM}$ and e) $\dot{V}_c=1\text{ LPM}$.

8) S_{gen} at $T_{h,i}=80\text{ }^{\circ}\text{C}$ results:

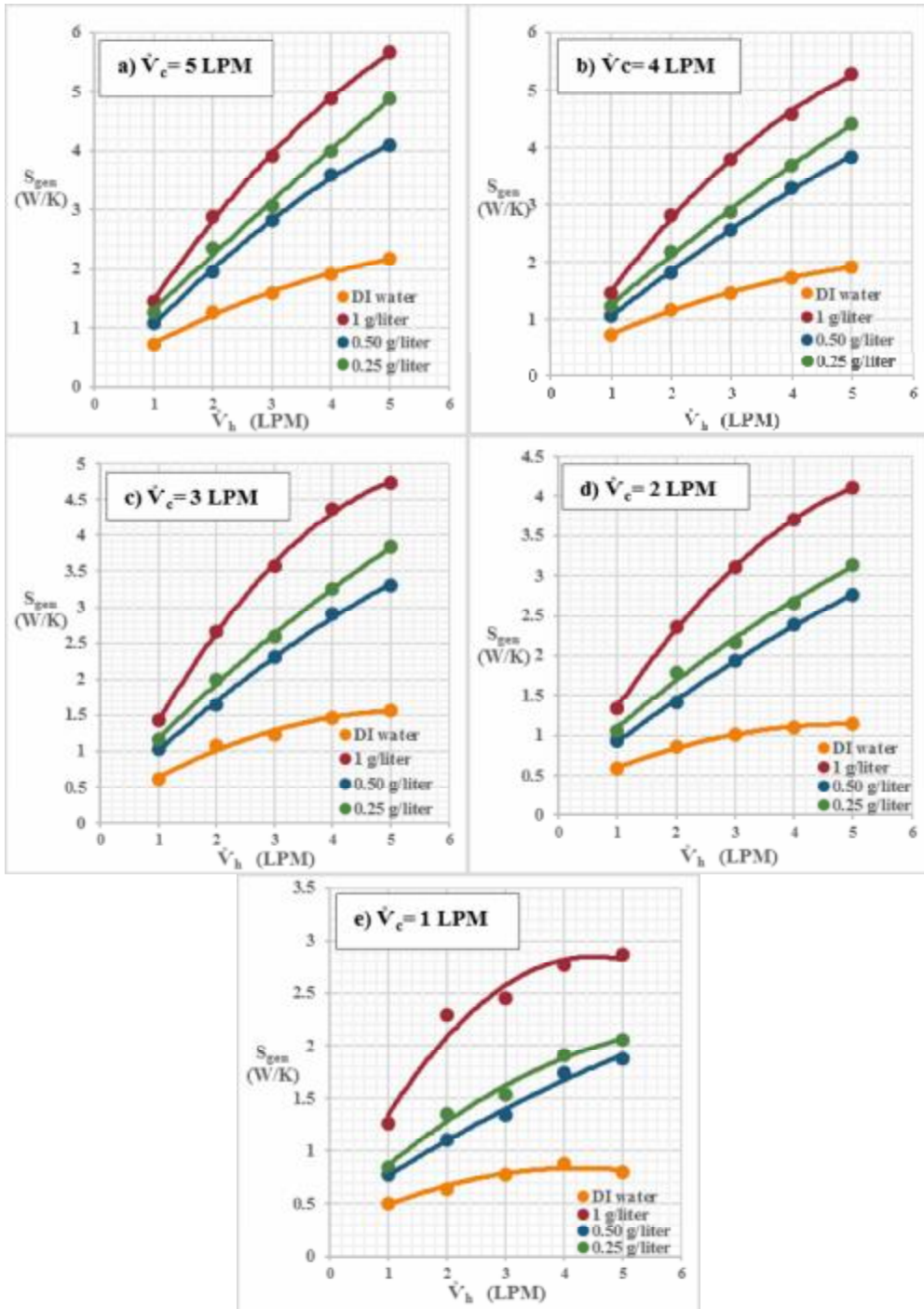


Figure (12): Variation of S_{gen} with volume flow rate of Nano-DI water, at $T_{h,i}=80\text{ }^{\circ}\text{C}$, at a) $\dot{V}_c= 5\text{ LPM}$, b) $\dot{V}_c= 4\text{ LPM}$, c) $\dot{V}_c= 3\text{ LPM}$, d) $\dot{V}_c= 2\text{ LPM}$ and e) $\dot{V}_c= 1\text{ LPM}$.

CONCLUSION:

The total entropy generation " S_{gen} " increases, with the increase of the volume flow rate of the hot fluid side. Moreover, the total entropy generation increases, by increasing the inlet temperature of the hot fluid side. Moreover, the total entropy generation decreases with decreasing the volume flow rates of the cold fluid side. Moreover, the total entropy generation increases, by increasing the Nano particles concentration in the DI water, except for the 0.5 g/liter, it shows lower values for the total entropy generation. Moreover, the 1 g/liter Nano-DI water reaches 155% increase over the DI water, at 80°C .

REFERENCES

1. Wen, D., Lin, G., Vafaei, S., and Zhang, K. (2009). Review of nanofluids for heat transfer applications. *Particuology*, 7(2), 141-150.
2. Choi, S. U. S. (1995). Enhancing thermal conductivity of fluids with nanoparticles. *ASME-Publications-Fed*, 231, 99-106.
3. Huang, D., Wu, Z., and Sunden, B. (2016). Effects of hybrid nanofluid mixture in plate heat exchangers. *Experimental Thermal and Fluid Science*, 72, 190-196.
4. Safi, M. A., Ghozatloo, A., Hamidi, A. A., and Shariaty-Niassar, M. (2014). Calculation of Heat Transfer Coefficient of MWCNT-TiO₂ Nanofluid in Plate Heat Exchanger. *International Journal of Nanoscience and Nanotechnology*, 10(3), 153-162.
5. Kabeel, A. E., El Maaty, T. A., and El Samadony, Y. (2013). The effect of using nano-particles on corrugated plate heat exchanger performance, *Applied Thermal Engineering*, 52(1), 221-229.
6. Ray, D. R., Das, D. K., and Vajjha, R. S. (2014). Experimental and numerical investigations of nanofluids performance in a compact minichannel plate heat exchanger. *International Journal of Heat and Mass Transfer*, 71, 732-746.
7. Fard, H., Talaie, M. R., and Nasr, S. (2011). Numerical and experimental investigation of heat transfer of zno/water nanofluid in the concentric tube and plate heat exchangers. *Thermal Science*, 15(1), 183-194.
8. Focke, W. W., Zachariades, J., & Olivier, I. (1985). The effect of the corrugation inclination angle on the thermohydraulic performance of plate heat exchangers. *International Journal of Heat and Mass Transfer*, 28(8), 1469-1479.
9. Godson, L., Raja, B., Lal, D. M., & Wongwises, S. (2010). Enhancement of heat transfer using nanofluids—an overview. *Renewable and sustainable energy reviews*, 14(2), 629-641
10. Lenert, A., & Wang, E. N. (2012). Optimization of nanofluid volumetric receivers for solar thermal energy conversion. *Solar Energy*, 86(1), 253-265.
11. Hordy, N., Rabilloud, D., Meunier, J. L., & Coulombe, S. (2014). High temperature and long-term stability of carbon nanotube nanofluids for direct absorption solar thermal collectors. *Solar Energy*, 105, 82-90.